
Improving Variational Inference with Inverse Autoregressive Flow

Diederik P. Kingma*, Tim Salimans* and Max Welling[×]

* OpenAI, San Francisco

[×] University of Amsterdam, University of California Irvine,
and the Canadian Institute for Advanced Research (CIFAR)
dpkingma@openai.com, tim@openai.com, M.Welling@uva.nl

Abstract

We propose a simple and scalable method for improving the flexibility of variational inference through a transformation with autoregressive networks.

Autoregressive networks, such as RNNs and MADE Germain et al. (2015), are very powerful models; however, ancestral sampling in such networks is a sequential operation, therefore unappealing for direct use as approximate posteriors in variational inference on parallel hardware such as GPUs. We find that by *inverting* autoregressive networks we can obtain equally powerful data transformations that can often be computed in parallel. We show that such data transformations, *inverse autoregressive flows* (IAF), can be used to transform a simple distribution over the latent variables into a much more flexible distribution, while still allowing us to compute the resulting variables' probability density function. The method is simple to implement, can be made arbitrarily flexible, and (in contrast with previous work) is naturally applicable to latent variables that are organized in multidimensional tensors, such as 2D grids or time series.

The method is applied to a novel deep architecture of variational auto-encoders. In experiments we demonstrate that autoregressive flow leads to significant performance gains when applied to variational autoencoders for natural images.

1 Introduction

Stochastic variational inference Blei et al. (2012); Hoffman et al. (2013) is a method for scalable posterior inference with large datasets using stochastic gradient ascent. It can be made especially efficient for continuous latent variables through a latent-variable reparameterization and inference networks, amortizing the cost, resulting in a highly scalable learning procedure (Kingma and Welling, 2013; Rezende et al., 2014; Salimans et al., 2014). When using neural networks for both the inference network and generative model, this results in class of models called variational auto-encoders (VAEs). In this paper we propose *inverse autoregressive flow*, a method for improving the flexibility of inference networks. The method is a special case of *normalizing flow* Rezende and Mohamed (2015) and is especially well-suited for convolutional generative models.

At the core of our proposed method lie autoregressive functions that are normally used for density estimation: functions that take as input a variable with some specified ordering such as multidimensional tensors, and output a mean and standard deviation for each element of the input variable conditioned on the previous elements. Examples of such functions are neural density estimators such as RNNs, NADE Larochelle and Murray (2011); Uria et al. (2013) and MADE (Germain et al., 2015) models. We show that such functions can be easily turned into nonlinear transformations of the input, with a very simple Jacobian determinant: the product of standard deviations. Since the transformation is flexible and the determinant known, it can be used to transform a tensor with relatively simple known density, into a new tensor with more complicated density that is still cheaply computable. In

contrast with most previous work on improving inference models, this transformation is well suited to high-dimensional tensor variables, such as spatio-temporally organized variables.

We demonstrate this method by improving inference networks of deep variational auto-encoders. In particular, we train deep variational auto-encoders with latent variables at multiple levels of the hierarchy, where each stochastic variable is a 3D tensor (a stack of featuremaps), and demonstrate that the method greatly improves performance.

2 Variational Inference and Learning

Let \mathbf{x} be a (set of) observed variable(s), \mathbf{z} a (set of) latent variable(s) and let $p(\mathbf{x}, \mathbf{z})$ be the parametric model of their joint distribution, called the *generative model* defined over the variables. Given a dataset $\mathbf{X} = \{\mathbf{x}^1, \dots, \mathbf{x}^N\}$ we typically wish to perform maximum marginal likelihood learning of its parameters, i.e. to maximize

$$\log p(\mathbf{X}) = \sum_{i=1}^N \log p(\mathbf{x}^{(i)}), \quad (1)$$

but in general this marginal likelihood is intractable to compute or differentiate directly for flexible generative models, e.g. when components of the generative model are parameterized by neural networks. A solution is to introduce $q(\mathbf{z}|\mathbf{x})$, a parametric *inference model* defined over the latent variables, and optimize the *variational lower bound* on the marginal log-likelihood of each observation \mathbf{x} :

$$\log p(\mathbf{x}) \leq \mathbb{E}_{q(\mathbf{z}|\mathbf{x})} [\log p(\mathbf{x}, \mathbf{z}) - \log q(\mathbf{z}|\mathbf{x})] = \mathcal{L}(\mathbf{x}; \theta) \quad (2)$$

where θ indicates the parameters of p and q models. Keeping in mind that Kullback-Leibler divergences $D_{KL}(\cdot)$ are non-negative, it's clear that $\mathcal{L}(\mathbf{x}; \theta)$ is a lower bound on $\log p(\mathbf{x})$ since it can be written as follows):

$$\mathcal{L}(\mathbf{x}; \theta) = \log p(\mathbf{x}) - D_{KL}(q(\mathbf{z}|\mathbf{x})||p(\mathbf{z}|\mathbf{x})) \quad (3)$$

There are various ways to optimize the lower bound $\mathcal{L}(\mathbf{x}; \theta)$; for continuous \mathbf{z} it can be done efficiently through a re-parameterization of $q(\mathbf{z}|\mathbf{x})$, see e.g. (Kingma and Welling, 2013; Rezende et al., 2014).

As can be seen from equation (3), maximizing $\mathcal{L}(\mathbf{x}; \theta)$ w.r.t. θ will concurrently maximize $\log p(\mathbf{x})$ and minimize $D_{KL}(q(\mathbf{z}|\mathbf{x})||p(\mathbf{z}|\mathbf{x}))$. The closer $D_{KL}(q(\mathbf{z}|\mathbf{x})||p(\mathbf{z}|\mathbf{x}))$ is to 0, the closer $\mathcal{L}(\mathbf{x}; \theta)$ will be to $\log p(\mathbf{x})$, and the better an approximation our optimization objective $\mathcal{L}(\mathbf{x}; \theta)$ is to our true objective $\log p(\mathbf{x})$. Also, minimization of $D_{KL}(q(\mathbf{z}|\mathbf{x})||p(\mathbf{z}|\mathbf{x}))$ can be a goal in itself, if we're interested in using $q(\mathbf{z}|\mathbf{x})$ for inference after optimization. In any case, the divergence $D_{KL}(q(\mathbf{z}|\mathbf{x})||p(\mathbf{z}|\mathbf{x}))$ is a function of our parameters through both the inference model and the generative model, and increasing the flexibility of either is generally helpful towards our objective.

Note that in models with multiple latent variables, the inference model is typically factorized into partial inference models with some ordering; e.g. $q(\mathbf{z}^a, \mathbf{z}^b|\mathbf{x}) = q(\mathbf{z}^a|\mathbf{x})q(\mathbf{z}^b|\mathbf{z}^a, \mathbf{x})$. We'll write $q(\mathbf{z}|\mathbf{x}, \mathbf{c})$ to denote such partial inference models, conditioned on both the data \mathbf{x} and a further context \mathbf{c} which includes the previous latent variables according to the ordering.

2.1 Requirements for Computational Tractability

Requirements for the inference model, in order to be able to efficiently optimize the bound, are that it is computationally cheap to (1) compute and differentiate its probability density $q(\mathbf{z}|\mathbf{x})$, and (2) to sample from, since these operations need to be performed for each datapoint in a minibatch at every iteration of optimization. If \mathbf{z} is high-dimensional and we want to make efficient use of parallel computational resources like GPUs, then (3) parallelizability of these operations across dimensions of \mathbf{z} is a large factor towards efficiency. These three requirements restrict the class of approximate posteriors $q(\mathbf{z}|\mathbf{x})$ that are practical to use. In practice this often leads to the use of diagonal posteriors, e.g. $q(\mathbf{z}|\mathbf{x}) \sim \mathcal{N}(\mu(\mathbf{x}), \sigma^2(\mathbf{x}))$, where $\mu(\mathbf{x})$ and $\sigma(\mathbf{x})$ are often nonlinear functions parameterized by neural networks. However, as explained above, we also need the density $q(\mathbf{z}|\mathbf{x})$ to be sufficiently flexible to match the true posterior $p(\mathbf{z}|\mathbf{x})$.

2.2 Normalizing Flow

Normalizing Flow (NF), investigated by (Rezende and Mohamed, 2015) in the context of stochastic gradient variational inference, is a powerful framework for building flexible posterior distributions through an iterative procedure. The general idea is to start off with an initial random variable with a simple distribution, and then apply a series of invertible parameterized transformations \mathbf{f}^t , such that the last iterate \mathbf{z}^T has a more flexible distribution:

$$\mathbf{z}^0 \sim q(\mathbf{z}^0|\mathbf{x}, \mathbf{c}), \quad \mathbf{z}^t = \mathbf{f}^t(\mathbf{z}^{t-1}, \mathbf{x}, \mathbf{c}) \quad \forall t = 1 \dots T \quad (4)$$

As long as the Jacobian determinant of each of the transformations \mathbf{f}^t can be computed, we can still compute the probability density function of the last iterate:

$$\log q(\mathbf{z}^T|\mathbf{x}, \mathbf{c}) = \log q(\mathbf{z}^0|\mathbf{x}, \mathbf{c}) - \sum_{t=1}^T \log \det \left| \frac{d\mathbf{f}^t(\mathbf{z}^{t-1}, \mathbf{x}, \mathbf{c})}{d\mathbf{z}^{t-1}} \right| \quad (5)$$

However, (Rezende and Mohamed, 2015) experiment with only a very limited family of such invertible transformation with known Jacobian determinant, namely:

$$\mathbf{f}^t(\mathbf{z}^{t-1}) = \mathbf{z}_{t-1} + \mathbf{u}h(\mathbf{w}^T \mathbf{z}^{t-1} + b) \quad (6)$$

where \mathbf{u} and \mathbf{w} are vectors, \mathbf{w}^T is \mathbf{w} transposed, b is a scalar and $h(\cdot)$ is a nonlinearity, such that $\mathbf{u}h(\mathbf{w}^T \mathbf{z}_{t-1} + b)$ can be interpreted as an MLP with a bottleneck hidden layer with a single unit. Since information goes through the single bottleneck, a series of many such transformations is required to capture high-dimensional dependencies.

Another approach, taken by (Dinh et al., 2014), is to transform the data using shearing transformations, which have a fixed Jacobian matrix determinant of one. Typically, this type of transformations updates half of the latent variables $\mathbf{z}^{1, \dots, D/2}$ per step by adding a vector $\delta(\mathbf{z}^{D/2+1, \dots, D})$ which is a parameterized function of the remaining latent variables $\mathbf{z}^{D/2+1, \dots, D}$ which are kept fixed. Such a transformation admits completely general transformations $\delta(\cdot)$, but the requirement to partition the set of latent variables is still very limiting. Indeed, (Rezende and Mohamed, 2015) find that this type of transformation is generally less powerful than the normalizing flow presented above.

A potentially more powerful transformation is the *Hamiltonian flow* used in Hamiltonian Variational Inference (Salimans et al., 2014). Here, a transformation is generated by simulating the flow of a Hamiltonian system consisting of the latent variables \mathbf{z} , and a set of auxiliary variables. This type of transformation has the additional benefit that it is guided by the exact posterior distribution, and that it leaves this distribution invariant for small step sizes. Such a transformation could thus take us arbitrarily close to the exact posterior distribution if we can apply it for a sufficient number of times. In practice, however, Hamiltonian Variational Inference is very demanding computationally. Also, it requires an auxiliary variational bound to account for the auxiliary variables, which can impede progress if the bound is not sufficiently tight.

So far, no single method has been proposed that is both powerful and computationally cheap, and that satisfies all three of the computational tractability criteria of section 2.1.

3 Autoregressive Whitening of Data

In order to find a type of normalizing flow that is both powerful and computationally cheap, we consider a conceptually simple family of autoregressive Gaussian generative models which we will now briefly introduce. Let $\mathbf{y} = \{y_i\}_{i=1}^D$ be some random vector (or tensor) with some ordering on its elements. On this vector we define an autoregressive Gaussian generative model:

$$\begin{aligned} y_0 &= \mu_0 + \sigma_0 \cdot z_0, \\ y_i &= \mu_i(\mathbf{y}_{1:i-1}) + \sigma_i(\mathbf{y}_{1:i-1}) \cdot z_i, \\ z_i &\sim \mathcal{N}(0, 1) \quad \forall i, \end{aligned} \quad (7)$$

where $\mu_i(\mathbf{y}_{1:i-1})$ and $\sigma_i(\mathbf{y}_{1:i-1})$ are general functions, e.g. neural networks with parameters θ , that take the previous elements of \mathbf{y} as input and map them to a predicted mean and standard deviation for each element of \mathbf{y} . Models of this type include LSTMs (Hochreiter and Schmidhuber,

1997) predicting a mean and/or variance over input data, and (locally connected or fully connected) Gaussian MADE models (Germain et al., 2015). This is a rich class of very powerful models, but the disadvantage of using autoregressive models for variational inference is that the elements y_i have to be generated sequentially, which is slow when implemented on a GPU.

The autoregressive model effectively transforms the vector $\mathbf{z} \sim \mathcal{N}(0, \mathbf{I})$ to a vector \mathbf{y} with a more complicated distribution. As long as we have $\sigma_i > 0 \forall i$, this type of transformation is one-to-one, and can be inverted using

$$z_i = \frac{y_i - \mu_i(\mathbf{y}_{1:i-1})}{\sigma_i(\mathbf{y}_{1:i-1})}. \quad (8)$$

This inverse transformation *whitens* the data, turning the vector \mathbf{y} with complicated distribution back into a vector \mathbf{z} where each element is independently identically distributed according to the standard normal distribution. This inverse transformation is equally powerful as the autoregressive transformation above, but it has the crucial advantage that the individual elements z_i can now be calculated in parallel, as the z_i do not depend on each other given \mathbf{y} . The transformation $\mathbf{y} \rightarrow \mathbf{z}$ can thus be completely vectorized:

$$\mathbf{z} = (\mathbf{y} - \mu(\mathbf{y})) / \sigma(\mathbf{y}), \quad (9)$$

where the subtraction and division are elementwise. Unlike when using the autoregressive models naively, the *inverse* autoregressive transformation is thus both powerful *and* computationally cheap making this type of transformation appropriate for use with variational inference.

A key observation, important for variational inference, is that the autoregressive whitening operation explained above has a lower triangular Jacobian matrix, whose diagonal elements are the elements of $\sigma(\mathbf{y})$. Therefore, the log-determinant of the Jacobian of the transformation is simply minus the sum of the log-standard deviations used by the autoregressive Gaussian generative model:

$$\log \det \left| \frac{d\mathbf{z}}{d\mathbf{y}} \right| = - \sum_{i=1}^D \log \sigma_i(\mathbf{y}) \quad (10)$$

which is computationally cheap to compute, and allows us to evaluate the variational lower bound.

4 Inverse Autoregressive Flow (IAF)

As a result, we can use inverse autoregressive transformations (eq. (9)) as a type of normalizing flow (eq. (5)) for variational inference, which we call *inverse autoregressive flow* (IAF). If this transformation is used to match samples from an approximate posterior to a prior $p(\mathbf{z})$ that is standard normal, the transformation will indeed whiten, but otherwise the transformation can produce very general output distributions.

When using inverse autoregressive flow in our posterior approximation, we use a factorized Gaussian distribution for $\mathbf{z}^0 \sim q(\mathbf{z}^0 | \mathbf{x}, \mathbf{c})$, where the context \mathbf{c} contains the previous latent variables. We then perform T steps of IAF:

$$\text{for } t = 1 \dots T : \quad \mathbf{z}^t = \mathbf{f}^t(\mathbf{z}^{t-1}, \mathbf{x}, \mathbf{c}) = (\mathbf{z}^{t-1} - \mu^t(\mathbf{z}^{t-1}, \mathbf{x}, \mathbf{c})) / \sigma^t(\mathbf{z}^{t-1}, \mathbf{x}, \mathbf{c}), \quad (11)$$

where at every step we use a differently parameterized autoregressive model $\mathcal{N}(\mu^t, \sigma^t)$. If these models are sufficiently powerful, the final iterate \mathbf{z}^T will have a flexible distribution that can be closely fitted to the true posterior. Some examples are given below.

4.1 Linear IAF

Perhaps the simplest special case of IAF is the transformation of a Gaussian variable with diagonal covariance to one with linear dependencies.

Any full-covariance multivariate Gaussian distribution with mean \mathbf{m} and covariance matrix \mathbf{C} can be expressed as an autoregressive model with

$$\begin{aligned} y_i &= \mu_i(\mathbf{y}_{1:i-1}) + \sigma_i(\mathbf{y}_{1:i-1}) \cdot z_i, \text{ with} \\ \mu_i(\mathbf{y}_{1:i-1}) &= m_i + \mathbf{C}[i, 1 : i-1] \mathbf{C}[1 : i-1, 1 : i-1]^{-1} (\mathbf{y}_{1:i-1} - \mathbf{m}_{1:i-1}), \text{ and} \\ \sigma_i(\mathbf{y}_{1:i-1}) &= \mathbf{C}[i, i] - \mathbf{C}[i, 1 : i-1] \mathbf{C}[1 : i-1, 1 : i-1]^{-1} \mathbf{C}[1 : i-1, i]. \end{aligned}$$

Inverting the autoregressive model then gives $\mathbf{z} = (\mathbf{y} - \mu(\mathbf{y})) / \sigma(\mathbf{y}) = \mathbf{L}(\mathbf{y} - \mathbf{m})$ with \mathbf{L} the inverse Cholesky factorization of the covariance matrix \mathbf{C} .

By making $\mathbf{L}(\mathbf{x})$ and $\mathbf{m}(\mathbf{x})$ part of our variational encoder we can then use this inverse flow to form a posterior approximation. In experiments, we do this by starting out with a fully-factorized Gaussian approximate posterior as in e.g. (Kingma and Welling, 2013): $\mathbf{y} = \mu(\mathbf{x}) + \sigma(\mathbf{x}) \odot \epsilon$ where $\epsilon \sim \mathcal{N}(0, \mathbf{I})$, and where $\mu(\mathbf{x})$ and $\sigma(\mathbf{x})$ are vectors produced by our inference network. We then let the inference network produce an extra output $\mathbf{L}(\mathbf{x})$, the lower triangular inverse Cholesky matrix, which we then use to update the approximation. With this setup, the problem is overparameterized, so we define the mean vector \mathbf{m} above to be the zero vector, and we restrict \mathbf{L} to have ones on the diagonal. One step of linear IAF then turns the fully-factorized distribution of \mathbf{y} into an arbitrary multivariate Gaussian distribution: $\mathbf{z} = \mathbf{L}(\mathbf{x}) \cdot \mathbf{y}$. This results in a simple and computationally efficient posterior approximation, with scalar density function given by $q(\mathbf{z}|\mathbf{x}) = q(\mathbf{y}|\mathbf{x})$. By optimizing the variational lower bound we then fit this conditional multivariate Gaussian approximation to the true posterior distribution.

4.2 Nonlinear IAF through Masked Autoencoders (MADE)

For introducing nonlinear dependencies between the elements of \mathbf{z} , we specify the autoregressive Gaussian model $\mu_\theta, \sigma_\theta$ using the family of deep masked autoencoders (Germain et al., 2015). These models are arbitrarily flexible neural networks, where masks are applied to the weight matrices in such a way that the output $\mu(\mathbf{y}), \sigma(\mathbf{y})$ is autoregressive, i.e. $\partial\mu_i(\mathbf{y})/\partial y_j = 0, \partial\sigma_i(\mathbf{y})/\partial y_j = 0$ for $j \geq i$. Such models can implement very flexible densities, while still being computationally efficient, and they can be specified in either a fully connected (Germain et al., 2015), or convolutional way (van den Oord et al., 2016).

In experiments, we use one or two iterations of IAF with masked autoencoders, with reverse variable ordering in case of two iterations. The initial iterate, \mathbf{z}^0 , is the sample from a diagonal Gaussian posterior (like in (Kingma and Welling, 2013)). In each iteration of IAF, we then compute the mean and standard deviation through its masked autoencoder, and apply the transformation of equation (11). The final variable will have a highly flexible distribution, which we use as our variational posterior. For CIFAR-10, we use convolutional MADE van den Oord et al. (2016) with zero, one or two hidden layers.

4.3 Nonlinear IAF through Recurrent Neural Networks

Another method of parameterizing the $\mu_\theta, \sigma_\theta$ that define our inverse autoregressive flow are LSTMs and other recurrent neural networks (RNNs). These are generally more powerful than the masked autoencoder models, as they have an unbounded context window in computing the conditional means and variances. The downside of RNNs is that computation of $(\mu_\theta, \sigma_\theta)$ cannot generally be parallelized well, relative to masked autoencoder models. New methods have recently been developed to ameliorate these difficulties (van den Oord et al., 2016), and such methods could also be useful for the application we consider here.

5 Experiments

Code for reproducing key empirical results is available online¹; please refer to this code for architectural details. We empirically demonstrate the usefulness of inverse autoregressive flow for variational inference by training ResNet VAEs on the MNIST data set of handwritten digits and the CIFAR-10 data set of small natural images.

5.1 MNIST Architecture

In this experiment we follow a similar implementation of the convolutional VAE as in (Salimans et al., 2014) with some modifications, mainly that the encoder and decoder are parameterized with ResNet (He et al., 2015) blocks. For MNIST, the encoder consists of 3 sequences of two ResNet blocks each, the first sequence acting on 16 feature maps, the others on 32 feature maps. The first two sequences are followed by a 2-times subsampling operation implemented using 2×2 stride, while

¹<https://github.com/openai/iaf>

Table 1: Generative modeling results on binarized MNIST. Shown are averages; the number between brackets are standard deviations across different optimization runs. The right column shows an importance sampled estimate of the marginal likelihood for each model. Full covariance is implemented through linear IAF.

Posterior	s/epoch	$\log p(\mathbf{x}) \geq$	$\log p(\mathbf{x}) \approx$
Diagonal covariance	25.5	-85.6 (± 0.04)	-82.2 (± 0.03)
Full covariance	30.0	-84.3 (± 0.03)	-81.4 (± 0.03)
IAF	27.8	-84.0 (± 0.15)	-81.4 (± 0.14)

the third sequence is followed by a fully connected layer with 450 units. The decoder has a similar architecture, but with reversed direction. For optimization we use Adamax (Kingma and Ba, 2014), with learning rate $\alpha = 0.002$ and Polyak averaging (Polyak and Juditsky, 1992) to compute the final parameters.

We compared three forms of posteriors: a diagonal Gaussian, a full-covariance Gaussian (linear IAF) and nonlinear IAF through masked MLPs.

5.2 MNIST Results

Table 1 shows results on MNIST for these types of posteriors. As clear from these results, the full covariance Gaussian greatly improves upon the diagonal Gaussian. The nonlinear autoregressive flow slightly improves upon this result in terms of the lower bound, but doesn't differ significantly in terms of the marginal likelihood.

5.3 CIFAR-10 Architecture

For CIFAR-10, we used a neural architecture with ResNet units and multiple stochastic layers. Specifically, to train deep variational autoencoders on images, we utilize *pre-activation residual units* He et al. (2015) with single-hidden-layer residual functions. Our architecture consists of L stacked blocks, where each block ($l = 1..L$) is a combination of a bottom-up residual unit for inference, producing a series of bottom-up inputs \mathbf{h}_q^l , and a top-down residual unit used for both inference and generation, producing a series of top-down inputs \mathbf{h}_p^l . The hidden layer of each residual function in the generative model contains a combination of the usual deterministic hidden units and a relatively small number of stochastic hidden units with a heteroscedastic diagonal Gaussian distribution $p(\mathbf{z}^l | \mathbf{h}_p^l)$ given the unit's input \mathbf{h}_p^l , followed by a nonlinearity. Instead of ReLU nonlinearities, we use ELU Clevert et al. (2015) nonlinearities everywhere, giving better empirical results. We also found that the noise introduced by batch normalization hurts performance, and we avoid superfluous noise by replacing batch normalization with the weight normalization (Salimans and Kingma, 2016) method. We initialized the parameters using the data-dependent technique described in (Salimans and Kingma, 2016).

5.3.1 Bottom-Up Versus Top-Down

We compare a number of inference procedures; each either bottom-up, or top-down (see also Salimans (2016); Kaae Sønderby et al. (2016)). In case of bottom-up inference, latent variables are sampled in bottom-up order; part of the hidden layer of the residual function is stochastic, and forms the approximate posterior, $q(\mathbf{z}^l | \mathbf{h}_p^{l+1})$, conditioned on the bottom-up residual unit's input. The sample from this distribution is then, after application of the nonlinearity, treated as part of the hidden layer of the bottom-up residual function and thus used upstream.

In case of top-down inference, we first perform a fully deterministic bottom-up pass, before sampling from the posterior in top-down order. In this case, the approximate posterior for each layer is conditioned on both the bottom-up input and top-down input: $q(\mathbf{z}^l | \mathbf{h}_q^l, \mathbf{h}_p^l)$. The sample from this distribution is, again after application of the nonlinearity, treated as part of the hidden layer of the top-down residual function and thus used downstream.

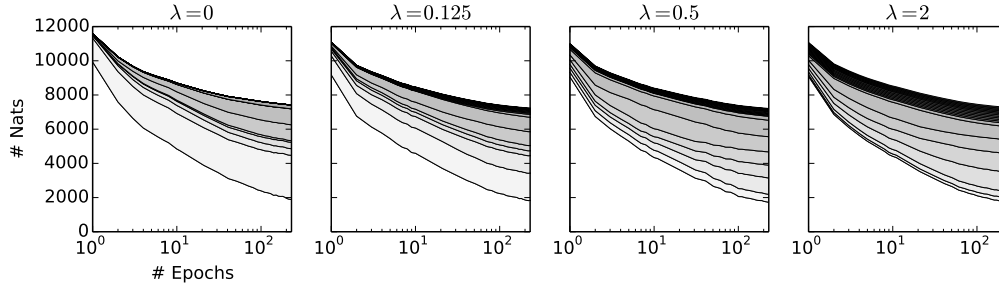


Figure 1: Shown are stack plots of the number of nats required to encode the CIFAR-10 set images, per stochastic layer of the 24-layer network, as a function of the number of training epochs, for different choices of minimum information constraint λ (see section 5.3.4). Enabling the constraint ($\lambda > 0$) results in avoidance of undesirable stable equilibria, and fuller use of the stochastic layers by the model. The bottom-most (white) area corresponds to the bottom-most (reconstruction) layer, the second area from the bottom denotes the first stochastic layer, the third area denotes the second stochastic layer, etc.

The approximate posteriors $q(\mathbf{z}^l | \cdot)$ are defined either through a diagonal Gaussian, or through an IAF posterior. In case of IAF, the context \mathbf{c} is provided by either \mathbf{h}_q^l , or \mathbf{h}_q^l and \mathbf{h}_p^l , dependent on inference direction.

We use either diagonal Gaussian posteriors, or IAF with a single step of convolutional MADE van den Oord et al. (2016) with zero, one or two layers of hidden layers with ELU nonlinearities Clevert et al. (2015). Note that IAF through MADE without hidden layers corresponds to a linear transformation; i.e. a Gaussian with off-diagonal covariance. In IAF, we investigate the importance of rescaling in the transformation, versus just the translation.

5.3.2 Subsampling / Upsampling

The first layer of the encoder is a convolutional layer with 2×2 subsampling; the last layer of the decoder has a matching 2×2 upsampling. The ResNet layers are divided into 4 levels with each an equal number of layers. The first layer of each level in the encoder performs 2×2 downsampling in its first operation; the matching convolution in the decoder has a matching 2×2 upsampling operation. Downsampling and upsampling of identity connections is done through nearest-neighbour. Downsampling in convolutional layers is done through strided convolution, while upsampling is done by a regular convolution producing $4 \times$ the number of features and a reshaping operation.

5.3.3 Discretized Logistic Likelihood

The first layer of the encoder, and the last layer of the decoder, consist of convolutions that project from/to input space. The pixel data is scaled to the range $[0, 1]$, and the data likelihood of pixel values in the generative model is the probability mass of the pixel value under the logistic distribution. Noting that the CDF of the standard logistic distribution is simply the sigmoid function, we simply compute the probability mass per input pixel using $p(x_i | \mu_i, s_i) = \text{CDF}(x_i + \frac{1}{256} | \mu_i, s_i) - \text{CDF}(x_i | \mu_i, s_i)$, where the locations μ_i are output of the decoder, and the log-scales $\log s_i$ are learned scalar parameter per input channel.

5.3.4 Objective with a Minimum Information Constraint

To accelerate optimization and reach better optima, we optimize the bound using a slightly modified objective with a minimum information constraint. Consistent with findings in Bowman et al. (2015) and Kaae Sønderby et al. (2016), we found that stochastic optimization with the unmodified lower bound objective often gets stuck in an undesirable stable equilibrium. At the start of training, the likelihood term $\log p(\mathbf{x} | \mathbf{z})$ is relatively weak, such that an initially attractive state is where $q(\mathbf{z} | \mathbf{x}) \approx p(\mathbf{z})$. In this state, encoder gradients have a relatively low signal-to-noise ratio, resulting in a stable equilibrium from which it is difficult to escape. The solution proposed in (Bowman et al.,

Table 2: Our results in *average number of bits per data dimension* on the test set with ResNet VAEs, for various choices of posterior ResNet depth, and IAF depth. The top-down posterior of (Kaae Sønderby et al., 2016; Salimans, 2016) resulted in numerical instabilities with deep ResNets.

Posterior:	ResNet Depth:		
	4	8	16
Bottom-up, factorized Gaussians	3.86	3.69	3.60
Bottom-up, IAF with 0 hidden layers	3.79	3.74	3.62
Bottom-up, IAF with 1 hidden layer	3.79	3.74	3.62
Top-Down (Kaae Sønderby et al., 2016)	5.44	5.43	-
Top-Down, factorized Gaussians	3.87	3.66	3.57
Top-Down, IAF with 0 hidden layers	3.74	3.66	3.60
Top-Down, IAF with 1 hidden layer	3.69	3.61	3.54



Figure 2: Random samples from learned generative model of CIFAR-10

2015) and (Kaae Sønderby et al., 2016) is to use an optimization schedule where the weight of the latent cost $D_{KL}(q(\mathbf{z}|\mathbf{x})||p(\mathbf{z}))$ is slowly annealed from 0 to 1 over many epochs.

We propose a different solution that does not depend on an annealing schedule, but uses a modified objective function that is constant throughout training instead. We divide the latent dimensions into the K subsets within which parameters are shared (e.g. the latent featuremaps, or individual dimensions if no parameter are shared across dimensions). We then use the following objective, which ensures that using less than λ nats of information per subset j (on average per minibatch \mathcal{M}) is not advantageous:

$$\tilde{\mathcal{L}}_\lambda = \mathbb{E}_{\mathbf{x} \sim \mathcal{M}} [\mathbb{E}_{q(\mathbf{z}|\mathbf{x})} [\log p(\mathbf{x}|\mathbf{z})]] - \sum_{j=1}^K \text{maximum}(\lambda, \mathbb{E}_{\mathbf{x} \sim \mathcal{M}} [D_{KL}(q(\mathbf{z}_j|\mathbf{x})||p(\mathbf{z}_j))]) \quad (12)$$

Since increasing the latent information is generally advantageous for the first (unaffected) term of the objective (often called the *negative reconstruction error*), this results in $\mathbb{E}_{\mathbf{x} \sim \mathcal{M}} [D_{KL}(q(\mathbf{z}_j|\mathbf{x})||p(\mathbf{z}_j))] \geq \lambda$ for all j , in practice.

We experimented with $\lambda \in [0, 0.125, 0.25, 0.5, 1, 2, 4, 8]$ and found that values in the range $\lambda \in [0.125, 0.25, 0.5, 1, 2]$ resulted in more than 0.1 nats improvement in bits/pixel on the CIFAR-10 benchmark.

Table 3: Our results with ResNet VAEs on CIFAR-10 images, compared to earlier results, in *average number of bits per data dimension* on the test set.

Method	bits/dim \leq
<i>Earlier results with tractable likelihood models:</i>	
Uniform distribution (van den Oord et al., 2016)	8.00
Multivariate Gaussian (van den Oord et al., 2016)	4.70
NICE (Dinh et al., 2014)	4.48
Deep GMMs (van den Oord and Schrauwen, 2014)	4.00
Real NVP (Dinh et al., 2016)	3.49
Pixel CNN van den Oord et al. (2016)	3.14
Pixel RNN (Row LSTM) van den Oord et al. (2016)	3.07
Pixel RNN (Diagonal BiLSTM) van den Oord et al. (2016)	3.00
<i>Earlier results with variationally trained latent-variable models:</i>	
Deep Diffusion (Sohl-Dickstein et al., 2015)	4.20
Convolutional DRAW (Gregor et al., 2016)	3.58
<i>Our results with ResNet VAEs:</i>	
Conditionally factorized Gaussian posteriors	3.51
IAF posteriors with 2 hidden layers	3.28

5.4 CIFAR-10 Results

To compare various choices of approximate posteriors and model depths, we trained ResNet VAEs for various choices of approximate posteriors; see table 2 for results. Please see our code for details. See our code for details.

Results improved further using architectural tweaks: using wide ResNets Zagoruyko and Komodakis (2016), using IAF with more hidden layers, and fewer up/downsampling layers. Please see our code for details. See table 3 for a comparison to previously reported results. Our architecture with IAF outperforms all earlier latent-variable architectures. We suspect that our approach can be competitive with the Pixel RNN through further advances in the architecture of the encoders, decoders and autoencoders used in IAF.

6 Conclusion

We presented *inverse autoregressive flow* (IAF), a method to make the posterior approximation for variational inference more flexible, thereby improving the variational lower bound. By inverting the sequential data generating process of an autoregressive Gaussian model, inverse autoregressive flow gives us a data transformation that is both very powerful and computationally efficient: the transformation has a tractable Jacobian determinant, and it can be vectorized for implementation on a GPU. By applying this transformation to the samples from our approximate posterior we can move their distribution closer to the exact posterior.

We empirically demonstrated the usefulness of inverse autoregressive flow for variational inference by training a novel deep architecture of variational auto-encoders. In experiments we demonstrated that autoregressive flow leads to significant performance gains compared to similar models with factorized Gaussian approximate posteriors, and we report the best results on CIFAR-10 for latent-variable models so far.

Acknowledgements

We thank Karol Gregor and Ilya Sutskever for fruitful discussions.

References

- Blei, D. M., Jordan, M. I., and Paisley, J. W. (2012). Variational Bayesian inference with Stochastic Search. In *Proceedings of the 29th International Conference on Machine Learning (ICML-12)*, pages 1367–1374.
- Bowman, S. R., Vilnis, L., Vinyals, O., Dai, A. M., Jozefowicz, R., and Bengio, S. (2015). Generating sentences from a continuous space. *arXiv preprint arXiv:1511.06349*.
- Clevert, D.-A., Unterthiner, T., and Hochreiter, S. (2015). Fast and accurate deep network learning by Exponential Linear Units (ELUs). *arXiv preprint arXiv:1511.07289*.
- Dinh, L., Krueger, D., and Bengio, Y. (2014). Nice: non-linear independent components estimation. *arXiv preprint arXiv:1410.8516*.
- Dinh, L., Sohl-Dickstein, J., and Bengio, S. (2016). Density estimation using Real NVP. *arXiv preprint arXiv:1605.08803*.
- Germain, M., Gregor, K., Murray, I., and Larochelle, H. (2015). Made: Masked autoencoder for distribution estimation. *arXiv preprint arXiv:1502.03509*.
- Gregor, K., Besse, F., Rezende, D. J., Danihelka, I., and Wierstra, D. (2016). Towards conceptual compression. *arXiv preprint arXiv:1604.08772*.
- He, K., Zhang, X., Ren, S., and Sun, J. (2015). Deep residual learning for image recognition. *arXiv preprint arXiv:1512.03385*.
- Hochreiter, S. and Schmidhuber, J. (1997). Long Short-Term Memory. *Neural computation*, 9(8):1735–1780.
- Hoffman, M. D., Blei, D. M., Wang, C., and Paisley, J. (2013). Stochastic variational inference. *The Journal of Machine Learning Research*, 14(1):1303–1347.
- Kaae Sønderby, C., Raiko, T., Maaløe, L., Kaae Sønderby, S., and Winther, O. (2016). How to train deep variational autoencoders and probabilistic ladder networks. *arXiv preprint arXiv:1602.02282*.
- Kingma, D. and Ba, J. (2014). Adam: A method for stochastic optimization. *arXiv preprint arXiv:1412.6980*.
- Kingma, D. P. and Welling, M. (2013). Auto-encoding variational Bayes. *Proceedings of the 2nd International Conference on Learning Representations*.
- Larochelle, H. and Murray, I. (2011). *The Neural Autoregressive Distribution Estimator*. AISTATS.
- Polyak, B. T. and Juditsky, A. B. (1992). Acceleration of stochastic approximation by averaging. *SIAM Journal on Control and Optimization*, 30(4):838–855.
- Rezende, D. and Mohamed, S. (2015). Variational inference with normalizing flows. In *Proceedings of The 32nd International Conference on Machine Learning*, pages 1530–1538.
- Rezende, D. J., Mohamed, S., and Wierstra, D. (2014). Stochastic backpropagation and approximate inference in deep generative models. In *Proceedings of the 31st International Conference on Machine Learning (ICML-14)*, pages 1278–1286.
- Salimans, T. (2016). A structured variational auto-encoder for learning deep hierarchies of sparse features. *arXiv preprint arXiv:1602.08734*.
- Salimans, T. and Kingma, D. P. (2016). Weight normalization: A simple reparameterization to accelerate training of deep neural networks. *arXiv preprint arXiv:1602.07868*.
- Salimans, T., Kingma, D. P., and Welling, M. (2014). Markov chain Monte Carlo and variational inference: Bridging the gap. *arXiv preprint arXiv:1410.6460*.
- Sohl-Dickstein, J., Weiss, E. A., Maheswaranathan, N., and Ganguli, S. (2015). Deep unsupervised learning using nonequilibrium thermodynamics. *arXiv preprint arXiv:1503.03585*.
- Uribe, B., Murray, I., and Larochelle, H. (2013). RNAE: The real-valued neural autoregressive density-estimator. In *Advances in Neural Information Processing Systems*, pages 2175–2183.
- van den Oord, A., Kalchbrenner, N., and Kavukcuoglu, K. (2016). Pixel recurrent neural networks. *arXiv preprint arXiv:1601.06759*.
- van den Oord, A. and Schrauwen, B. (2014). Factoring variations in natural images with deep gaussian mixture models. In *Advances in Neural Information Processing Systems*, pages 3518–3526.
- Zagoruyko, S. and Komodakis, N. (2016). Wide residual networks. *arXiv preprint arXiv:1605.07146*.